Orientational transitions of anisotropic nanoparticles at liquid–liquid interfaces

2007 J. Phys.: Condens. Matter 19 375110

(http://iopscience.iop.org/0953-8984/19/37/375110)

IOP PUBLISHING JOURNAL OF PHYSICS: CONDENSED MATTER

J. Phys.: Condens. Matter **19** (2007) 375110 (12pp) doi:10.1088/0953-8984/19/37/375110

Orientational transitions of anisotropic nanoparticles at liquid–liquid interfaces

Fernando Bresme[1] **and Jordi Faraudo**[2]

[1] Department of Chemistry, Imperial College, London SW7 2AZ, UK
[2] Departmento de Física, Universidad Autónoma de Barcelona, E-08193 Bellaterra, Barcelona, Spain

Received 18 October 2006, in final form 5 December 2006
Published 13 August 2007
Online at stacks.iop.org/JPhysCM/19/375110

Abstract

We investigate the behaviour of ellipsoidal nanoparticles adsorbed at liquid–liquid interfaces and under the influence of an external field. We propose a simple thermodynamic model that predicts the equilibrium orientation of the particles as a function of the field strength and the interfacial tensions. We show that the interplay of particle geometry, particle size and field strength results in discontinuous orientational transitions, which are characterized by a discontinuous change of the particle orientation at a specific field strength. We also introduce a Monte Carlo methodology to investigate the orientational behaviour of anisotropic nanoparticles at interfaces. The simulation results show that the theory very accurately predicts the behaviour of anisotropic nanoparticles at intermediate field strengths.

(Some figures in this article are in colour only in the electronic version)

1. Introduction

Microparticles and nanoparticles adsorbed at liquid–liquid or liquid–air interfaces show a behaviour similar to that observed in surfactants [1]. In his pioneering work Pieranski showed that microparticles can adsorb very strongly at the water–air interface, forming two-dimensional colloidal crystals [2]. The activation energy associated to the detachment of particles from high surface tension interfaces, such as water–air, is very high, and shows a strong dependence with particle size: $10^7\ k_BT$ for microparticles and 10–$10^2\ k_BT$ for nanoparticles. It has been shown that the activation energy can be rather sensitive to interfacial forces such as the line tension, when the particles become very small. Hence, the line tension can trigger wetting–drying transitions in solid particles adsorbed at interfaces [3–7], as well as in small sessile drops adsorbed at solid surfaces [9]. Very recently, we have shown that nanoparticle stability at liquid–liquid interfaces is strongly dependent on the particle geometry [7, 8]. Thus ellipsoidal nanoparticles exhibit a reduced stability with respect to oblate nanoparticles, their stability being also more sensitive to line tension effects. Our

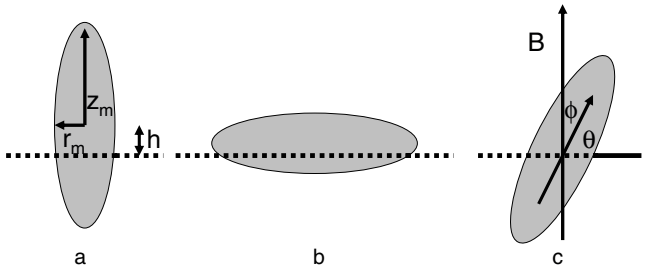

Figure 1. Sketch of an ellipsoidal nanoparticle adsorbed at a liquid–liquid interface, in vertical (a), horizontal (b) and tilted (c) configuration. The variables defining the geometry and orientation of the particle are discussed in the text.

results suggest that the nanoparticle shape can be used as an efficient variable to control the particle adsorption energy. This notion could find applications in the design of nanoparticles with surface properties that enable a better control of the stability of emulsions and foams, for instance.

Most experimental and theoretical works devoted to particles at interfaces have focused on spherical particles. Nonetheless, recent advances in materials science have provided new routes to make particles of different shapes [11, 12, 10]. These new methods have made possible the investigation of anisotropic microparticles at interfaces. Recent experiments using ellipsoidal particles have shown important differences between the behaviour of anisotropic particles and their spherical counterparts [13]. In addition to the modification of the particle shape, it is also possible to add specific functionality to the particles [14]. Such particles can interact with external fields (electric or magnetic), opening new routes to control their behaviour at interfaces. Recent work has shown that the use of external fields offers an efficient route to induce alignment of fibres in liquid suspensions [15] and self-assembly of spherical particles at interfaces [16–18]. One can speculate that the coupling of external fields and particle geometry can result in new physical behaviour. In this paper we address this issue. We investigate the behaviour of one ellipsoid nanoparticle at a liquid–liquid interface in the presence of an external field.

The paper is structured as follows. First, we introduce a simple thermodynamic model that accounts for the interaction of the nanoparticle with an external field that induces changes in the nanoparticle orientation. The theory is applied to investigate the physical behaviour of anisotropic nanoparticles as a function of their aspect ratio and field strength. We introduce a Monte Carlo (MC) simulation methodology to investigate nanoparticles in the presence of an external field. A summary, with the main conclusions and further remarks, closes the paper.

2. Thermodynamics of anisotropic particles at interfaces

The system we want to investigate consists of an ellipsoidal particle adsorbed at a liquid–liquid interface (see figure 1). The free energy function for anisotropic particles at interfaces has been derived by us in a previous work [7]. We showed that the coupling of particle geometry and the line tension results in a complex phenomenology.

In the following we consider particles of very small dimensions (nanometres to micrometres), i.e., dimensions much smaller than the capillary length of the interface. Consequently we neglect gravity effects in the remainder of the paper. For our discussion it is convenient to introduce first the free energy function for one particle in the absence of an external field.

2.1. Ellipsoids at interfaces: zero-field conditions

The free energy of a system consisting of one particle at a liquid–liquid interface (at constant temperature, volume and number of particles), can be written as

$$F_{\text{int}} = -\gamma_{12}A_{st} + (\gamma_{2p} - \gamma_{1p})A_{2p} + \tau L, \tag{1}$$

where γ_{ij} are the interfacial tensions of the different interfaces (particle–liquid and liquid–liquid), A_{ij} are the corresponding interfacial areas, A_{st} is the area of intersection of the particle with the interface, τ is the line tension of the three-phase line, and L is the length of the three-phase line. Equation (1) gives the free energy of the particle at the interface relative to the free energy of the particle in one of the liquid phases. An equation similar to (1) has been used to investigate the behaviour of spherical particles [3].

We provided in our previous work explicit expressions for the free energies of ellipsoids in two orientations: one in which the major axis is parallel to the interface plane, and a second one in which it is normal to the interface [7]. We will refer to these orientations as *horizontal* and *vertical* configurations, respectively. The free energy of the ellipsoidal particle can be expressed in terms of a set of variables that define the geometry of the particle. Hence the major z_m and minor r_m axes of the ellipsoid define the aspect ratio, α, and the eccentricity, ε, which, for prolate shaped particles ($\alpha \geqslant 1$), are given by

$$\alpha = \frac{z_m}{r_m} \tag{2}$$

$$\varepsilon = \sqrt{1 - \alpha^{-2}}. \tag{3}$$

The total surface area of the ellipsoid, $A_p = A_{1p} + A_{2p}$, is defined by

$$A_p = 4\pi r_m^2 G(\alpha), \tag{4}$$

where $G(\alpha)$ is the geometrical aspect ratio, which again for prolate objects ($\alpha \geqslant 1$) is given by

$$G(\alpha) = \frac{1}{2} + \frac{1}{2}\frac{\alpha}{\varepsilon}\arcsin\varepsilon. \tag{5}$$

Using the equation above it is possible to derive explicit expressions for the free energy of the particles in the horizontal and vertical configurations. The final equations are given in the appendix.

In our previous work we investigated in detail the dependence of the free energy of anisotropic particles with the line tension [7]. In this work we are interested in the free energy difference between horizontal and vertical configurations and its dependence on an applied external field (see below). We therefore ignore line tension effects as a starting point. From equations (A.1) and (A.3) it is easy to see that the most stable configuration in the absence of any external field is the horizontal one, since this configuration maximizes the area removed from the liquid–liquid interface. The difference in the free energy of the horizontal and vertical configurations increases with the aspect ratio, α. Hence the larger α, i.e., the more anisotropic the particle, the less stable is the vertical configuration with respect to the horizontal one. Figure 2 illustrates this idea for a representative situation, $\gamma_{1p} = \gamma_{2p}$ and $\tau = 0$. Since the surface tension of the particle with both liquids is the same, the particle does have the same preference for both liquids, and it is adsorbed with its centre of mass at the interface, i.e., $\overline{h} = 0$, with $\overline{h} = h/z_m$ for the vertical configuration and $\overline{h} = h/r_m$ for the horizontal one (see the minima in figure 1). The free energy minima obtained from equations (A.1) and (A.3) (see figure 2) provide an estimate of the activation energy needed to detach anisotropic particles from the interface. For a particle of size $r_m = 2$ nm and aspect ratio $\alpha = 1.666$ adsorbed at an interface with interfacial tension of the order of 50 mN m^{-1} ($\approx$water–oil interface), this

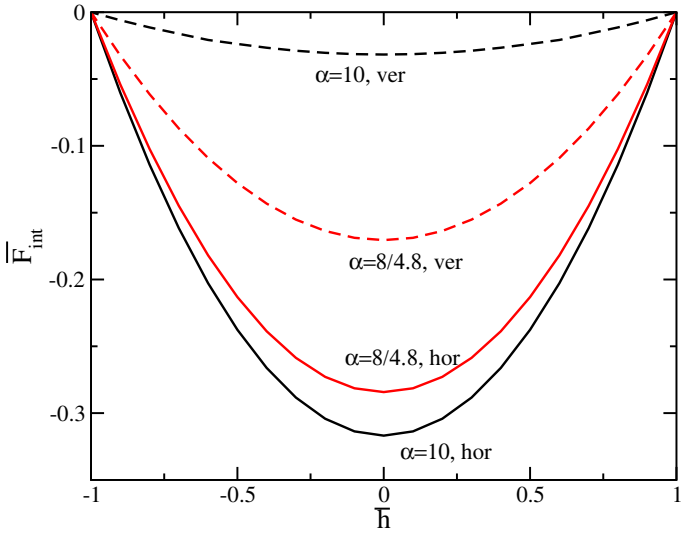

Figure 2. Free energy ($\overline{F} = F/(\gamma_{12}A_p)$) of the ellipsoidal nanoparticle as a function of its position, $\overline{h}$, at the interface for $\gamma_{1p} = \gamma_{2p}$, $\tau = 0$. Full lines represent the free energy of particles in the horizontal ('hor') configuration and dashed lines, particles in vertical ('ver') configuration.

gives an activation energy of the order of 10^2 and 2×10^2 k_BT ($T = 298$ K), for vertical and horizontal configurations respectively. This result shows that these small particles are very strongly adsorbed at the interface. We can also estimate the free energy difference between horizontal and vertical orientations. Considering the example above, we get a free energy difference of $\approx 10^2$ k_BT for $\alpha = 1.6666$, whereas for more anisotropic particles, $\alpha = 10$, the differences increases up to $\approx 10^3$ k_BT. The free energy differences are very large, showing that it is very unlikely to find particles in the vertical orientation. Nonetheless, it is important to note that the free energy difference strongly depends on the interfacial tension. For low surface tension interfaces, $\gamma_{12} \approx 1$ mN m^{-1}, the differences in free energy are dramatically reduced, ≈ 10 k_BT for $\alpha = 1.6666$, suggesting that an external perturbation, such as a magnetic or electrostatic field, could stabilize the vertical orientation with respect to the horizontal one. We analyse this situation below.

2.2. Particles at interfaces under an external field

In the following we consider ellipsoidal particles adsorbed at the interface under the influence of an external field. We assume that the field is normal to the interface and interacts with the particle through an embedded electrostatic or magnetic permanent dipole, whose direction coincides with the major axis of the ellipsoid. The resulting torque will tend to align the dipole with the applied field, inducing a change in the orientation of the ellipsoid, from horizontal to vertical. The external field adds a contribution to the free energy of the particle at the interface. We assume this is of the type $F_{ext} = -\vec{\mu} \cdot \vec{H}$, where $\vec{\mu}$ and $\vec{H}$ are the dipole and the field respectively. For simplicity we will express the external field contribution as $F_{ext} = -B\cos\phi$, where $B = |\vec{\mu}||\vec{H}|$ represents the field–dipole strength, and ϕ is the angle between the field and dipole vectors. The free energy of the particle at the interface can be written as

$$F_{int} = -\gamma_{12}A_{st} + (\gamma_{2p} - \gamma_{1p})A_{2p} + \tau L - B\cos\phi. \tag{6}$$

According to our definitions, $\phi = 0$ corresponds to the particle in the vertical orientation, whereas $\phi = \pi/2$ corresponds to the particle in the horizontal configuration.

To illustrate the effect of the external field we consider a situation in which the particle rotates around its centre of mass, which is located at the interface plane. This corresponds to the case $\gamma_{1p} \approx \gamma_{2p}$. Moreover, we neglect the effect of the line tension as a first approximation. The line tension is expected to have a significant effect on the wetting properties of the nanoparticle only when the interfacial tension is very low, and when the three-phase line has a large curvature [4–6]. We assume that the particle sizes and interfacial tensions are large enough, so that the line tension has a small influence. Finally, we approximate the three-phase line around the nanoparticle as an ellipse. Using these approximations in equation (6) we obtain a simpler expression,

$$F_{\text{int}} = -\gamma_{12} A_{st} - B\cos(\phi), \tag{7}$$

that can be used to investigate the effect of the external field on the particle orientation. The area, A_{st}, in the equation above is the area of intersection of the particle with the interface and is given by

$$A_{st} = r_m \pi \sqrt{\frac{z_m^2 r_m^2}{r_m^2 \cos^2(\theta) + z_m^2 \sin^2(\theta)}}, \tag{8}$$

where θ is the angle that the major axis of the particle (i.e. the dipole) makes with the interface (see figure 1(c)), and it is related to ϕ through, $\phi = \pi/2 - \theta$. Using these definitions in equation (7) we obtain the following expression for the free energy,

$$\overline{F}_{\text{int}}(\theta) = \frac{F_{\text{int}}(\theta)}{A_p \gamma_{12}} = -\frac{\alpha}{4G(\alpha)} \sqrt{\frac{1}{\cos^2(\theta) + \alpha^2 \sin^2(\theta)}} - \frac{B\cos(\pi/2 - \theta)}{A_p \gamma_{12}}, \tag{9}$$

where again the total area of the ellipsoid is given by equation (4).

Figure 3 shows the free energy of the ellipsoid as a function of its orientation. The external field imposes a preferred orientation to the particle, which tends to align with the field direction. For a given field the equilibrium orientation (defined by the free energy minimum) is strongly dependent on the particle aspect ratio. The less anisotropic the particle the larger the effect of the field. For particles with small anisotropy the stable configuration is the vertical one, i.e., the particle aligns with the field. Obviously, in the limit of an spherical particle, the vertical orientation would be the preferred one, even for an external field of negligible strength. For particles with intermediate anisotropy the field will result in a configuration in which the particle is tilted at an angle θ to the interface. For very large anisotropies it becomes harder to tilt the particle and this is reflected in the very small changes in the equilibrium angle with respect to the zero-field condition ($\theta = 0$) (see figure 3).

Interestingly, the thermodynamic model given in equation (9) suggests that the change in the orientation of the particle, from the horizontal to the vertical orientation, occurs in a discontinuous way. Hence, there is critical field strength at which the particle 'jumps' from a tilted configuration to a vertical one. This is illustrated in figure 4, which shows the free energy curves for a representative aspect ratio and different field strengths. Thus, depending on the field strength we can have a free energy curve with a single minimum, which corresponds to the particle having a tilted configuration, or a free energy curve with two minima, which suggest an equilibrium between the tilted configuration and the vertical one. These two configurations are nonetheless separated by an energy barrier. Therefore the transition from one configuration to the other is an activated process. The magnitude of the energy barrier varies with particle dimensions and interfacial tension. For instance, for a particle of size $r_m \approx 2$ nm, and aspect ratio $\alpha = 1.6666$, adsorbed at an interface with interfacial tension of 50 mN m^{-1} (oil–water),

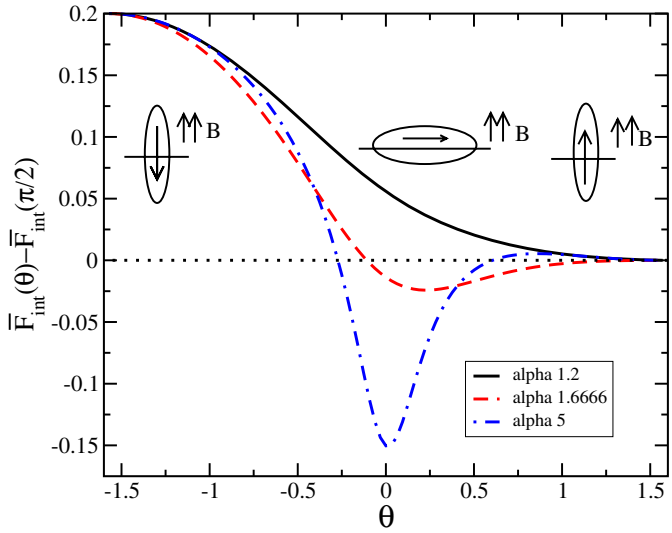

Figure 3. Free energy of the ellipsoidal nanoparticle as a function of its orientation, θ, at the interface. The results correspond to a representative field strength, $\overline{B} = 0.1$, and different particle aspect ratio: $\alpha = 1.2$ (full line), $\alpha = 1.6666$ (dashed line), $\alpha = 5$ (dot–dashed line).

the activation energy would be $\approx 2.5\ k_B T$. For larger particles, $r_m = 5$ or 30 nm, the activation energy increases to $\approx 16\ k_B T$ and $\approx 600\ k_B T$ respectively. Consequently, small particles will be able to sample both conformations, 'tilted' and 'vertical', but large particles will be trapped in the tilted or vertical conformations. If we increase the field further we reach a critical field strength, B_c, for which there is not local minimum for the tilted configuration. For this field strength the particle 'jumps' discontinuously from the tilted to the vertical orientation, where the nanoparticle dipole points in the direction of the field (cf figure 4). This physical behaviour corresponds to a discontinuous orientational transition, and it is one of the main results of the simple model described above.

The behaviour of the particle with the external field is summarized in figure 5, which represents the variation of the equilibrium angle, θ, with the field strength. The equilibrium angles were obtained by minimizing the free energy in equation (9) at constant field strength. Figure 5 clearly illustrates the existence of the discontinuous orientational transition. As discussed above, the variation of the tilt angle with the field is strongly dependent on the particle aspect ratio. For particles with small anisotropy the transition occurs for angles that are very close to the vertical orientation, and finally the transition disappears in the limit of a spherical particle.

In the following section we explore the orientational behaviour of ellipsoids at liquid–liquid interfaces using Monte Carlo simulations.

3. Computer simulations of non-spherical particles at interfaces

Simulations of a single non-spherical particle adsorbed at the interface between two immiscible liquids, I and J, were performed using Monte Carlo simulations in the canonical ensemble (NVT). Liquid particles of the same species interact through the truncated and shifted Lennard-Jones potential,

$$u_{ii}(r) = u_{jj}(r) = 4\varepsilon \left[\left(\frac{\sigma}{r}\right)^{12} - \left(\frac{\sigma}{r}\right)^{6} \right] - u_{\text{cut}}, \tag{10}$$

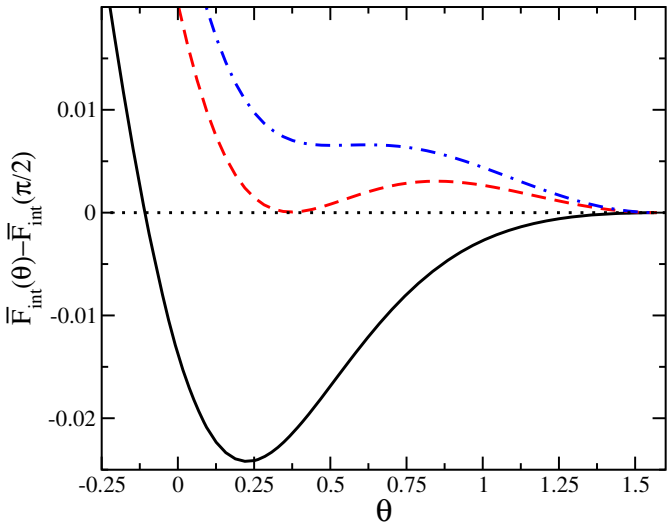

Figure 4. Free energies of an ellipsoidal nanoparticle with aspect ratio $\alpha = 1.6666$, as a function of its orientation at the interface. The lines represent external fields of different strengths: $\overline{B} = 0.1$ (full line), $\overline{B} = 0.134$ (dashed line), and $\overline{B} = 0.145$ (dot–dashed line). The latter is the critical field that results in the orientational transition (see text for details).

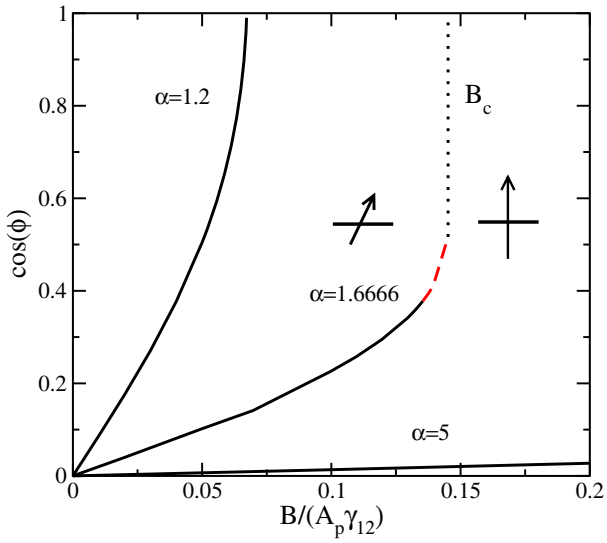

Figure 5. Variation of the particle orientation ($\cos\phi$) with the external field. The different lines correspond to particles of different aspect ratio. The dashed line for $\alpha = 1.6666$ corresponds to the region of metastability of the tilted configuration (see text for details).

where ε and σ represent the interaction strength and effective diameter of the particles respectively, and $u_{\rm cut}$ is the energy at the potential cutoff, $r_{\rm cut} = 2.5\sigma$. The interactions between particles of different species, ij, were modelled using a completely repulsive interaction,

$$u_{ij}(r) = 4\epsilon\left(\frac{\sigma}{r}\right)^{12} - u_{\rm cut}. \tag{11}$$

This interaction ensures that the liquid phases, I and J, are immiscible.

The anisotropic nanoparticle was modelled as an ellipsoid. The interactions between the nanoparticle and the liquid were computed using the Gay–Berne potential [19, 20],

$$u_{pf}(\vec{v},\vec{r}) = 4\epsilon_{pf}\left[\left(\frac{\sigma}{r-\sigma_{pf}(\vec{v},\vec{r})+\sigma}\right)^{12} - \left(\frac{\sigma}{r-\sigma_{pf}(\vec{v},\vec{r})+\sigma}\right)^{6}\right] - u_{\text{cut}}, \tag{12}$$

where $\vec{v}$ is a vector that defines the direction of the major axis of the ellipsoid and $\vec{r}$ is the vector joining the centre of mass of the nanoparticle and the centre of a given liquid particle. ϵ_{pf} and $\sigma_{pf}(\vec{v},\vec{r})$ are the interaction strength and the effective diameter of the liquid–nanoparticle interactions respectively, and u_{cut} is the potential energy at the cutoff distance, 2.5σ. The effective diameter is given by the following expression,

$$\sigma_{pf}(\vec{v},\vec{r}) = \sigma_{\perp}\left[1-\chi\left(\frac{\vec{r}\cdot\vec{v}}{|\vec{r}|\,|\vec{v}|}\right)^{2}\right]^{-1/2}, \tag{13}$$

where $\chi = (\sigma_{\parallel}^2 - \sigma_{\perp}^2)/\sigma_{\parallel}^2$, and $\sigma_{\parallel}^2$ and $\sigma_{\perp}^2$ define the nanoparticle dimensions and anisotropy. In this work we identify $\sigma_{\parallel}$ and $\sigma_{\perp}$ with the major, z_m, and minor, r_m, axes defined in section 2.

The ellipsoid–liquid interaction was set to $\epsilon_{pf} = 1.5\epsilon$ for both types of liquid particle, $f = i$ and j. This means that the nanoparticle has the same affinity for both liquids and effectively sits in the middle of the interface. This corresponds to the situation investigated in the previous section, where the nanoparticle rotates around its centre of mass, which is sitting at the interface. The nanoparticle aspect ratio was set to $\alpha = \sigma_{\parallel}/\sigma_{\perp} = 8/4.8 = 1.6666$. In addition to the liquid–liquid and liquid–particle interactions we considered an external potential, which imposes a preferred orientation to the nanoparticle with respect to the interface plane,

$$U_{\text{ext}}(\phi) = -B\cos\phi, \tag{14}$$

where ϕ is the angle between the dipole vector (which coincides with the major axis of the ellipsoid) and the field direction (normal to the interface). Again, B measures the strength of the external field.

In order to accommodate the nanoparticle at the liquid–liquid interface and minimize boundary condition effects [21] due to the finite size of the simulation box, we set the interface cross-sectional area to $L_y = L_z = 29.4\sigma$, whereas the simulation box in the direction normal to the interface was set to $L_x = 2L_y$, to ensure adequate formation of the fluid bulk phase away from the interface. This set-up results in very large system sizes. Typically our simulations involved over 3×10^4 particles. A standard simulation of such a large system showed itself to be very computationally inefficient. To speed up the simulations we resorted to the implementation of the *cell linked method* [22]. This method showed itself to be extremely efficient, reducing the computational time down to two orders of magnitude with respect to a non-optimized brute-force method.

The simulations typically involved 3×10^5 cycles. Each cycle consisted of N Monte Carlo steps, where N is the total number of particles. A Monte Carlo step consisted of an attempt to move the particle from its original position. In the case of the nanoparticle in addition to this, each step also included an attempt to change the orientation of the nanoparticle. New orientations were generated ensuring uniform sampling [23]. The Monte Carlo step was accepted according to the Metropolis criterion (see for instance [22]). The maximum displacement and maximum change in the orientation were selected so that ≈50% of the attempted moves were accepted.

The interface was created by putting together two preequilibrated liquid slabs. The simulations were then performed at a reduced temperature $T^* = k_{\text{B}}T/\epsilon = 1.0$. The bulk densities of the immiscible liquids are [6] $\rho_I^* = \rho_J^* = N\sigma^3/V = 0.690 \pm 0.002$, and

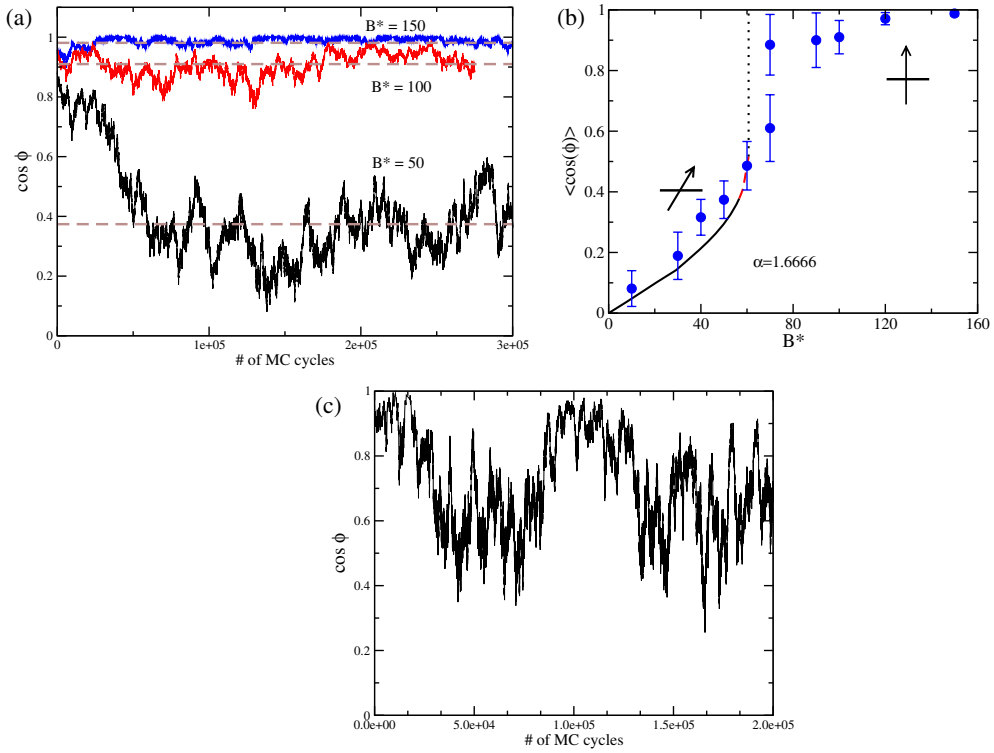

Figure 6. (a) Variation of the particle orientation with the number of Monte Carlo cycles. Results for different external fields, $B^* = 50$, 100 and 150, are shown. Horizontal lines represent the average orientation obtained from different runs. (b) Dependence of particle orientation with the external field: Monte Carlo simulation (symbols), and theoretical predictions from equation (9) (line). (c) Particle orientation as a function of the number of Monte Carlo cycles for the external field $B^* = 70$.

they were obtained from the analysis of the density profiles. We have considered the same liquid–liquid interface in simulations of spherical nanoparticles at interfaces [6]. Following our previous work the normal pressure and the interfacial tension for the thermodynamic state investigated here are $P_N^* = P\sigma^3/\epsilon = 0.44$ and $\gamma^* = \gamma\sigma^2/\epsilon = 1.04$ ($\approx$11 mN m^{-1} considering $\sigma = 3.405$ Å and $\epsilon/k_B = 119.8$ K) respectively.

Figure 6(a) shows representative results for the orientation of the nanoparticle as a function of the number of configurations. Our results show that the nanoparticle orientation (given by $\cos\phi$) fluctuates around a well-defined average. The equilibration can be rather slow, depending on the initial conditions. In some cases we required $\approx 5 \times 10^4$ cycles of equilibration (see $B^* = B/\epsilon = 50$ in figure 6(a)). Figure 6(b) shows the variation of the equilibrium angle with the external field. The errors in the simulation data are given as one standard deviation from the mean. The simulation results show that in order to induce an appreciable orientation in the small nanoparticles considered here $(\sigma_\parallel, \sigma_\perp) = (2.72, 1.632)$ nm (taking $\sigma = 0.3404$ nm) field energies of the order of $B = 40\, k_B T$ would be required.

Our simulation results for the nanoparticle offer the possibility to test the thermodynamic model discussed in the preceding section. We find that the thermodynamic model (equation (9)) predicts rather well the orientation of the ellipsoid for weak fields $B^* \leqslant 40$. This is despite the simplicity of the model, which ignores the molecular nature of the interface, and in particular

the interface finite thickness and interface thermal fluctuations. The simulation results seem to deviate slightly from the theory as the field strength is increased. For the particle simulated here, the thermodynamic model predicts a discontinuous change in the orientation at a field strength of $B^* = 61$. The simulations do not show such discontinuous change in the angle, but for $B^* = 70$ we find that the particle orientation alternates between two different angles (see figures 6(c) and (b)). The existence of two well-defined orientations is clearly shown in a histogram of the particle angle, which exhibits two distinctive maxima (not shown). The fact that during the simulations we can observe transitions from one orientation to the other indicates that the thermal barriers associated to the local minima are of the order of the thermal energy. Thus the simulations indicate that the thermal fluctuations play an important role in determining the orientation of the particle at the interface. These fluctuations that perturb the interfacial structure, and that are not included in the thermodynamic model, must influence the free energy landscape of the nanoparticle at the interface introducing deviations with respect to the predictions of the thermodynamic model. Nonetheless, despite these shortcomings, the theory provides a correct description of the general physical behaviour of the anisotropic nanoparticles at the interface.

4. Summary and final remarks

We have investigated the orientation of anisotropic nanoparticles at interfaces under the influence of an external field. We assume that the nanoparticles can interact with the field through an appropriate embedded electrostatic or magnetic dipole, which is parallel to the major axis of the ellipsoid. For zero-field conditions the stable configuration of the particle corresponds to the major axis lying in the interface plane. The interaction of the particle with the external field results in a torque that tends to align the dipole with the applied field, inducing a change in the orientation of the ellipsoid. We have introduced an analytical thermodynamic model that enables the calculation of the free energy of the particle at the interface in terms of the particle aspect ratio, particle size and external field.

One of the main results from this work is that the orientation of the nanoparticles with the external field is predicted to exhibit a discontinuous orientational transition. Hence, for a critical field strength the particle 'jumps' from a configuration in which the major axis (dipole moment) is tilted with respect to the interface plane to a vertical configuration, in which the major axis is aligned with the external field. The critical field needed to induce the transition is strongly dependent on the nanoparticle size, aspect ratio and interfacial tension. The more favourable conditions to observe the transitions predicted in this work correspond to superparamagnetic nanoparticles with intermediate anisotropies (major/minor axes $\approx 3/2$–2) at surfaces with low interfacial tensions. For example, for a typical superparamagnetic particle (magnetic susceptibility $\chi \approx 10$) with a major axis about 3000 nm and 1.6 anisotropy at an interface with a surface tension about 10 mN m^{-1} we obtain the orientational transition ($B/A_p\gamma_{12} = 0.15$) using a magnetic field of about 0.02 T. In the case of stronger magnetic fields (about 0.1 T), typical superparamagnetic particles have a saturation magnetic moment of about $\mu \approx 80$ A m^2 kg^{-1}, so orientational transitions can in principle be observed at a water/air interface ($\gamma_{12} \approx 73$ mN m^{-1}).

We have also reported Monte Carlo simulations of nanoparticles adsorbed at liquid–liquid interfaces in the presence of an external field. With this purpose we have introduced an efficient Monte Carlo simulation methodology that enables the investigation of anisotropic nanoparticles adsorbed at interfaces. The interactions between the nanoparticles and the liquid can be conveniently implemented using orientation-dependent potentials. Simulations of a small ellipsoidal particle (minor axis $\approx$2.7 nm and aspect ratio $\alpha = 1.6666$) show that the

simple theoretical model introduced in this work accurately describes the orientation of the particles for intermediate external fields. This is remarkable considering the simplicity of the theory, which ignores the molecular nature of the interface, and interfacial forces such as the line tension. We observe deviations for strong field conditions, suggesting that a quantitative description of this regime may require introducing other contributions in the theory, such as the finite size of the interface, interfacial fluctuations and possibly a more accurate representation of the three-phase line shape. Further simulations are required to unequivocally characterize the orientational transitions predicted by the theory. A modification of the simulation set-up, for instance, increasing the particle size or particle aspect ratio, should help to reach this objective.

The ideas presented here open a new perspective on the behaviour of anisotropic nanoparticles at interfaces. We believe that the orientational transitions and the general physical behaviour that we have described in this paper can provide new routes to design sensors, control the self-assembly of particles at interfaces, or develop new concepts for the manufacture of interfacial devices.

Acknowledgments

The authors would like to thank EPSRC (FB) and the Spanish and Catalan Ministry of Science (JF), Grant Nos FIS2006-12296-C02-01 and DGR 2005SGR00087, for financial support. Computer resources on HPCx were provided via the UK's HPC Materials Chemistry Consortium (EPSRC grant EP/D504872). We would like to acknowledge the Barcelona Supercomputer Center (Spain) for providing resources on the Mare Nostrum Supercomputer.

Appendix

In this appendix we provide explicit expressions for the free energy of ellipsoidal particles at interfaces. In the following we consider prolate particles, i.e., ellipsoids with aspect ratio $\alpha = z_m/r_m \geqslant 1$.

The free energy of an ellipsoid particle in the vertical configuration (major axis normal to the interface) is given by [7]

$$\overline{F}_{\rm int}^{\rm ver} = \frac{F_{\rm int}^{\rm ver}}{A_p\gamma_{12}} = -\frac{1}{4G}(1-\overline{h}^2) + \frac{\gamma_{2p}-\gamma_{1p}}{\gamma_{12}}\overline{A}_{2p}^{\rm ver}(\overline{h}) + \overline{\tau}\frac{1}{2\sqrt{G}}\sqrt{1-\overline{h}^2}, \tag{A.1}$$

where $\overline{h} = h/z_m$ describes the position of the centre of the particle relative to the interface (see figure 1), $\overline{\tau} = \tau/(\gamma_{12}\sqrt{A_p/(4\pi)})$ is the reduced line tension, and $\overline{A}_{2p}^{\rm ver}$ is the area of the particle immersed in phase 2. This area can be calculated from

$$\overline{A}_{2p}^{\rm ver} = \frac{A_{2p}^{\rm ver}}{A_p} = \frac{1}{2} - \frac{\alpha\overline{h}}{4G}\sqrt{1-\overline{h}^2\varepsilon^2} - \frac{\alpha\arcsin(\overline{h}\varepsilon)}{4\varepsilon G}, \tag{A.2}$$

where G is the geometrical aspect ratio defined in the main text (equation (5)).

The free energy for the ellipsoid in the horizontal configuration, i.e., with the major axis lying parallel to the interface is given by [7]

$$\overline{F}_{\rm int}^{\rm hor} = -\frac{\alpha}{4G}(1-\overline{h}^2) + \frac{\gamma_{2p}-\gamma_{1p}}{\gamma_{12}}\overline{A}_{2p}^{\rm hor}(\overline{h}) + \overline{\tau}\frac{1}{\pi\sqrt{G}}\max(\alpha,1)\sqrt{1-\overline{h}^2}E(\varepsilon), \tag{A.3}$$

where $\overline{h} = h/r_m$, $E(\varepsilon)$ is the complete elliptic integral of the second kind, and $\overline{A}_{2p}^{\rm hor} = A_{2p}^{\rm hor}/A_p$

is again the area of the ellipsoid immersed in phase 2, which is given by the integral [7]

$$A_{2p}^{\mathrm{hor}}(\overline{h}) = \frac{\alpha}{\pi G}\int_0^1 \mathrm{d}x''\sqrt{1-(1-\overline{h}^2)x''^2(1-\alpha^{-2})}\arctan\left[\frac{\sqrt{1-\overline{h}^2}\sqrt{1-x''^2}}{\overline{h}}\right] \tag{A.4}$$

with $x'' = x'/\sqrt{1-\overline{h}^2}$. This integral can be solved by numerical integration using a standard numerical method.

References

[1] Binks B P 2002 *Curr. Opin. Colloid Interface Sci.* **7** 21
[2] Pieranski P 1980 *Phys. Rev. Lett.* **45** 569
[3] Aveyard R and Clint J H 1996 *J. Chem. Soc. Faraday Trans.* **92** 85
[4] Bresme F and Quirke N 1998 *Phys. Rev. Lett.* **80** 3791
[5] Bresme F and Quirke N 1999 *J. Chem. Phys.* **110** 3536
[6] Bresme F and Quirke N 1999 *Phys. Chem. Chem. Phys.* **1** 2149
[7] Faraudo J and Bresme F 2003 *J. Chem. Phys.* **118** 6518
[8] Faraudo J and Bresme F 2004 *J. Non-Equilib. Thermodyn.* **29** 397
[9] Widom B 1995 *J. Phys. Chem.* **99** 2803
[10] Rees G D *et al* 1999 *Langmuir* **15** 1993
[11] Ho C C, Keller A, Odell J A and Ottewill R H 1993 *Colloid Polym. Sci.* **271** 469
[12] Snoeks E *et al* 2000 *Adv. Mater.* **12** 1511
[13] Loudet J C, Alsayed A M, Zhang J and Yodh A G 2005 *Phys. Rev. Lett.* **94** 018301
[14] Hyeon T 2003 *Chem. Commun.* 927
[15] Kimura T *et al* 2004 *Langmuir* **20** 5669
[16] Zhan K, Mendez-Alcaraz J M and Maret G 1997 *Phys. Rev. Lett.* **79** 175
[17] Zhan K, Lenke R and Maret G 1999 *Phys. Rev. Lett.* **82** 2721
[18] Froltsov V A, Blaak R, Likos C N and Lowen H 2003 *Phys. Rev.* E **68** 061406
[19] Gay J G and Berne B J 1981 *J. Chem. Phys.* **74** 3316
[20] Cleaver D J, Care C M, Allen M P and Neal M P 1996 *Phys. Rev.* E **54** 559
[21] González-Melchor M, Bresme F and Alejandre J 2005 *J. Chem. Phys.* **122** 104710
[22] Allen M P and Tildesley D J 1987 *Computer Simulation of Liquids* (Oxford: Clarendon)
[23] Marsaglia G 1972 *Ann. Mats. Stat.* **43** 645